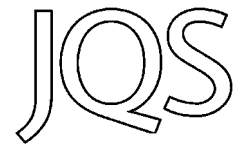


West Antarctica's Sensitivity to Natural and Human-forced Climate Change Over the Holocene



P. A. MAYEWSKI,^{1,2*} K. A. MAASCH,^{1,2} D. DIXON,^{1,2} S. B. SNEED,¹ R. OGLESBY,³
E. KOROTKIKH,^{1,2} M. POTOCKI,^{1,2} B. GRIGHOLM,^{1,2} K. KREUTZ,^{1,2} A. V. KURBATOV,^{1,2}
N. SPAULDING,^{1,2} J. C. STAGER,^{1,4} K. C. TAYLOR,⁵ E. J. STEIG,⁶ J. WHITE,⁷ N. A. N. BERTLER,⁸
I. GOODWIN,⁹ J. C. SIMÕES,¹⁰ R. JAÑA,¹¹ S. KRAUS¹² and J. FASTOOK^{1,13}

¹Climate Change Institute, University of Maine, Orono, ME, USA

²Department of Earth Sciences, University of Maine, Orono, ME, USA

³Department of Earth and Atmospheric Sciences and School of Natural Resources, University of Nebraska, Lincoln, NE, USA

⁴Natural Sciences, Paul Smith's College, Paul Smiths, NY, USA

⁵Desert Research Institute, University/Community College System Nevada, Reno, NV, USA

⁶Quaternary Research Center, University of Washington, Seattle, WA, USA

⁷Institute of Arctic and Alpine Research, University of Colorado, Boulder, CO, USA

⁸Joint Antarctic Institute, Victoria University and GNS Science, Wellington, New Zealand

⁹Department of Environment and Geography, Macquarie University, NSW, Australia

¹⁰Centro Polar e Climático, Universidade Federal do Rio Grande do Sul, Porto Alegre, Brazil

¹¹Instituto Antártico Chileno (INACH), Punta Arenas, Chile

¹²Servicio Nacional de Geología y Minería (SERNAGEOMIN), Santiago, Chile

¹³Department of Computer Sciences, University of Maine, Orono, ME, USA

Received 18 May 2012; Revised 4 September 2012; Accepted 14 September 2012

ABSTRACT: The location and intensity of the austral westerlies strongly influence southern hemisphere precipitation and heat transport with consequences for human society and ecosystems. With future warming, global climate models project increased aridity in southern mid-latitudes related to continued poleward contraction of the austral westerlies. We utilize Antarctic ice cores to investigate past and to set the stage for the prediction of future behaviour of the westerlies. We show that Holocene West Antarctic ice core reconstructions of atmospheric circulation sensitively record naturally forced progressive as well as abrupt changes. We also show that recent poleward migration of the westerlies coincident with increased emission of greenhouse gases and the Antarctic ozone hole has led to unprecedented penetration, compared with >100,000 years ago, of air masses bringing warmth, extra-Antarctic source dust and anthropogenic pollutants into West Antarctica. Copyright © 2012 John Wiley & Sons, Ltd.

KEYWORDS: abrupt climate change; Antarctica; anthropogenic activity; atmospheric circulation; ice cores.

Introduction

In recent decades, air temperatures over portions of coastal Antarctica, the Southern Ocean and the winter atmosphere over Antarctica have exhibited record warming (Gille, 2002; Turner *et al.*, 2006) with associated catastrophic disintegration of Antarctic ice shelves and coastal glaciers (Thomas *et al.*, 2008) and impacts on the marine ecosystem (Schofield *et al.*, 2010). Concurrently, there has been a strengthening of the austral westerlies (southern hemisphere westerlies), resulting from a steeper latitudinal (N–S) thermal gradient produced by the Antarctic ozone hole and increased tropospheric greenhouse gases (Thompson and Solomon, 2002) that has left much of interior Antarctica isolated from the full force of greenhouse gas warming and led to increases in sea ice extent surrounding much of Antarctica (Turner *et al.*, 2009a). Recent average latitudinal displacement and speed of the polar jet stream and associated westerlies has been significant, moving poleward (winter 3.3°S, summer 1.8°S) and intensifying (up to 6%) between 1981–1990 and 2001–2010 (Fig. 1).

Understanding climate change over Antarctica and the Southern Ocean is integrally tied to understanding changes in the austral westerlies (e.g. Divine *et al.*, 2009; Lamy *et al.*, 2010) and related major low-pressure features such as the Amundsen Sea Low (Turner *et al.*, 2009b; Mayewski *et al.*, 2009) as most of the heat and moisture transport through the mid to high latitudes is accomplished by variations in the

intensity, timing and location of atmospheric circulation systems. Climate change, particularly abrupt climate change, poses enormous socio-economic challenges and threatens ecosystem health. As an example, austral westerly winds and associated circulation features are primary sources of winter rainfall over southern South America, Africa, Australia and New Zealand. Understanding the timing and magnitude of changes in the austral westerlies is critical to predictions of future moisture flux availability.

Here we examine ice core-derived proxies for changes in atmospheric circulation developed from three deep ice cores: GISP2 (Greenland Ice Sheet Project Two; 3210 m a.s.l.), SD (Siple Dome; West Antarctica; 621 m a.s.l.; Fig. 1) and TD (Taylor Dome; East Antarctica; 2400 m a.s.l.; Fig. 1). These records provide well-dated climate proxy reconstructions for major atmospheric circulation features based on calibration with instrumented records. In the case of Antarctica, reconstructions are spatially verified by the ITASE (International Trans Antarctic Scientific Expedition) array of ice cores covering the last ~200–1000 ITASE a BP where BP refers to years (a) before AD 2000 (Fig. 1).

Ice core dating

Annual layer dating of the SD (Taylor *et al.*, 2004) and GISP2 (Meese *et al.*, 1997) ice cores over the Holocene is based on multi-parameter techniques such as electrical conductivity and visual stratigraphy and is calibrated using known volcanic events. Dating uncertainty for SD is conservatively estimated to

*Correspondence: P. A. Mayewski, ¹Climate Change Institute, as above
E-mail: paul.mayewski@maine.edu

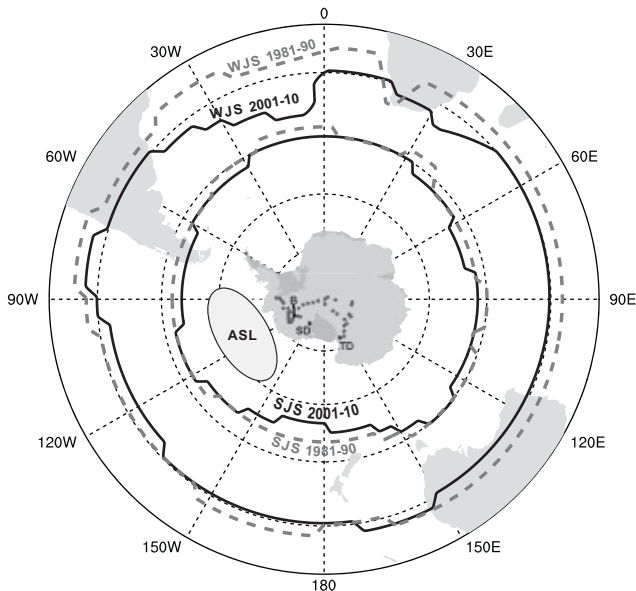


Figure 1. Location of Siple Dome (SD), Taylor Dome (TD), Byrd (B) and ITASE ice cores plus winter and summer range of the polar front associated with the austral westerlies and the Amundsen Sea Low. ASL refers to the general region encompassed by the Amundsen Sea Low. Also shown are the polar jet stream during summer (SJS) and winter (WJS) averaged over AD 1981–1990 (dashed) and AD 2001–2010 (solid). Jet position was estimated by identifying maxima of the 10-year average zonal wind for a latitude–height cross-section at each longitude of the NCEP reanalysis. Winter jet is at 200 mb and summer jet at 250 mb. Dots over Antarctica represent the location of International Trans Antarctic Scientific Expedition (ITASE) ice core sites used in this paper.

be < 5% from 0 to 2300 (SD a BP) and ~5% for the interval 2300–8600 (SD a BP) (Taylor *et al.*, 2004; Brook *et al.*, 2005). The reported dating uncertainty for GISP2 Holocene is 1% from 0 to 3289 (GISP2 a BP) and 2% from 3289 (GISP2 a BP) to the beginning of the Holocene (Meese *et al.*, 1997). The TD major chemistry record covers the Holocene, but with a resolution similar to SD and GISP2 only for the last ~3000 a. Vertical strain data available for the upper 130 m of the TD core (Hawley *et al.*, 2002) coupled with tephra analyses yield a timescale for the last 1300 a with an estimated dating uncertainty of 2–3% (Hawley *et al.*, 2002). Dating of the deglacial portion of the TD record at 15 800 (TD a BP) was adjusted to 17 800 (TD a BP) based on Ca^{2+} concentration tuning to the Dome C deep ice core (Mulvaney *et al.*, 2000). Annual layer dating for the ITASE ice core array is based on multi-parameter techniques including volcanic horizon calibration and is verified spatially across the West Antarctic ITASE ice core array (Dixon *et al.*, 2005).

Ice core–instrumented climate calibrations

We focus on co-registered (multiple measurements from the same sample) soluble ion concentrations using ion chromatography techniques identical to those described for the analysis of the GISP2 Holocene record (Mayewski *et al.*, 1997) and a numerical algorithm (O'Brien *et al.*, 1995) to estimate the marine sea-salt (ss) contribution and non-sea-salt (nss) continental dust contributions. We use the sea-salt species (represented by ssNa^+) and the continental dust species (represented by nssK^+ and nssCa^{2+}) to reconstruct the marine and continental source air masses, respectively, transported to SD, GISP2, TD and ITASE ice core sites. We use the marine productivity sourced methylsulfonate (MS^-) as a proxy for sea

ice extent. All values are reported as concentration rather than accumulation rate-adjusted flux to avoid confounding resultant values with accumulation rate multipliers that are significantly less precise than the chemical measurements. In support of this approach we note that no statistically meaningful associations have been identified that would allow sufficient understanding of the association between deposition style, snow accumulation rate and chemical concentration in our previous studies related to GISP2, TD, SD and ITASE ice cores, and hence the use of concentration (e.g. Dixon *et al.*, 2005).

Annually resolved ITASE, SD and GISP2 major ion time series were calibrated to modern instrumental climate records to develop atmospheric circulation proxy records as discussed below. Spatial representativeness of the instrumental calibrations is supported by multiple core calibrations available from the ITASE ice core array.

ssNa^+ proxy for atmospheric circulation

As all ssNa^+ is marine in origin concentrations in surface snow decrease with distance from the ocean, elevation above sea level and reduced intensity of transport (Legrand and Mayewski, 1997; Bertler *et al.*, 2005; Sneed *et al.*, 2011).

For GISP2, instrumental atmospheric surface pressure data over the North Atlantic and Asia from 1899 to 1987 were compared with annual GISP2 ssNa^+ and nssK^+ series to identify source regions and pressure–chemistry associations (Meeker and Mayewski, 2002). High (low) values of GISP2 ssNa^+ are significantly related (~75% of the variance of the shared first empirical orthogonal function) to below (above) average surface pressure in the Icelandic Low region of the North Atlantic. High (low) nssK^+ is statistically associated with higher (lower) average surface pressure in the Siberian High region.

Levels of ssNa^+ in the SD ice core are significantly influenced by the strength of the Amundsen Sea Low, a semi-permanent low-pressure system (Fig. 1) such that the linear correlation explains 25% of the ssNa^+ variance ($P < 0.001$) (Kreutz *et al.*, 2000). This association is shown in the correlation of SD ssNa^+ with Amundsen Sea surface pressure derived from the 2.5° latitude–longitude European Centre for Medium-Range Weather Forecasts numerical operational analyses and with the spring southern hemisphere Trans-Polar Index, a measure of Amundsen Sea Low strength over the period AD 1903–1994 (Kreutz *et al.*, 2000). SD surface pressure/ice core comparisons are spatially significant over much of West Antarctica as demonstrated using the ITASE ice core array such that when pressure is deeper (shallower) in the Amundsen Sea Low region (significantly correlated to ~10 mb of change), ssNa^+ concentrations increase (decrease) (Kaspari *et al.*, 2005).

Sources of ssNa^+ in Antarctic ice cores are also attributed to sea-salt spray from the open ocean and hence ice core ssNa^+ is interpreted as a proxy of atmospheric circulation over open marine sources. ssNa^+ is also present in ‘frost-flowers’ precipitated from the surface of freshly formed sea ice in coastal ice core sites (Rankin *et al.*, 2000). Studies over larger spatial areas such as West Antarctica using the ITASE cores suggest that frost-flower source ssNa^+ is localized to sites immediately adjacent to sea ice and has a minimal contribution to SD ssNa^+ (Kaspari *et al.*, 2005). Ultimately, the ssNa^+ reaching SD, assuming surface elevation remains constant, is associated with surface pressure in adjacent marine areas (Kreutz *et al.*, 2000; Kaspari *et al.*, 2005) and the question of whether the source of this ssNa^+ is from the open ocean or the sea ice surface does not impact the use of ice core ssNa^+ as a proxy for atmospheric circulation.

ssNa⁺, nssSO₄⁺ and MS⁻ proxies for sea ice extent

Using results stemming from the ITASE ice core array plus data from ice cores from the South Pole and Siple Dome, Sneed *et al.* (2011) investigated the use of MS⁻ as a proxy for Antarctic sea ice extent (SIE). Significant correlations greater than 90% exist between MS⁻ and mean SIE. Ice core–SIE calibrations also reveal that MS⁻ is associated with distance from the coast ($r = -0.42$, $P < 0.001$ (Bertler *et al.*, 2005) and SIE ($r = 0.82$, $P < 0.01$ for an ice core close to TD) (Welch *et al.*, 1993).

nssK⁺ and nssCa²⁺ proxies for atmospheric circulation

Source regions for crustal dust tracers such as nssK⁺ and nssCa²⁺ reaching Antarctica include: South America, Australia, New Zealand, South Africa and the ice-free areas of Antarctica. East Antarctic ice cores such as TD are believed to receive the majority of their crustal dust species from South America (Delmonte *et al.*, 2004). SD, because of its low elevation and position adjacent to the Amundsen Sea Low, is dominated by dust transported and mixed through the troposphere by the westerlies crossing Australia, New Zealand, South Africa and South America. Ice core–instrumental record calibration suggests that nssCa²⁺ is transported in the troposphere to SD and West Antarctica by the austral circumpolar zonal winds (Yan *et al.*, 2005). Intensification of the austral westerlies is therefore conducive to an increase in terrestrial dust transport to SD.

A recently developed climate proxy for dust-laden northerly air mass incursions (NAMIs) into central and western West Antarctica is based on the examination of 21 ITASE ice core nssCa²⁺ records (Dixon *et al.*, 2011a). SD and West Antarctic ITASE nssCa²⁺ is associated with modern changes in the austral westerlies and the Amundsen Sea Low revealed through correlation with the annual 850-mb zonal wind field in the area of the polar vortex ($r = > 0.45$, $P < 0.01$) resulting in a proxy for NAMIs containing extra-Antarctic dust (Dixon *et al.*, 2011a). The recent decadal rise in nssCa²⁺ at the more coastal ITASE sites is unprecedented for at least the last 200 a and is consistent with intensification of and the poleward contraction of the austral westerlies (Dixon *et al.*, 2011a) produced as a consequence of anthropogenic source greenhouse gas-induced warming and Antarctic ozone depletion (Thompson and Solomon, 2002). HYSPLIT air mass trajectory modeling and empirical orthogonal factor analysis combining atmospheric circulation reanalyses and dust loading records (Dixon *et al.*, 2011a) demonstrate that extra-Antarctic dusts reside in the austral westerlies belt for many days before entering West Antarctica through Amundsen Sea Low invasions (Dixon *et al.*, 2011a). The same authors demonstrate the importance of atmospheric circulation as the dominant factor controlling nssCa²⁺ concentrations in West Antarctica, surpassing the influence of drying in source regions as a source for the recent rise in nssCa²⁺.

We realize that ice core–instrumental calibrations may not always be stationary (Marshall *et al.*, 2009) and that calibrations with modern climate reanalysis data do not always imply constancy over the past, but we feel that it is: (i) essential to calibrate ice core records to develop climate proxies and that a large degree of constancy can be assumed as the basic physics of the climate system remains unchanged over time, and (ii) ice core climate calibrations can be tested by comparing consistency using multiple proxies and multiple ice cores as we do in this paper.

Together the GISP2, SD and TD ice cores provide a framework for assessing major periods of climate variability on a bi-polar transect from the North Atlantic (GISP2) to the

South Pacific and West Antarctica (SD), as well as incorporating the boundary between the Transantarctic Mountains and the East Antarctic plateau (TD).

West Antarctic climate diverges

To set the stage for understanding Holocene climate we first examine the last ~100 000 a using GISP2, SD and TD. Figure 2 shows that multi-millennial-scale variability in marine source seasalt (ssNa⁺) and terrestrial source dusts (nssCa²⁺ and nssK⁺) is similar in structure over much of the glacial portion of the records as previously demonstrated (Yiou *et al.*, 1997; Mulvaney *et al.*, 2000). In general, high concentrations of sea salts and continental dusts and significant millennial-scale variability characterize the last glacial period, followed during the Holocene by lower concentrations as climate variability is reduced, temperatures rise and continental dust sources decrease with rising sea level and increased moisture transport. There is, however, a marked difference in trend for West Antarctica (SD) and coastal East Antarctica (TD) compared with the North Atlantic (GISP2) starting ~9000–10 000 (SD a BP). Notably SD and TD ssNa⁺ start to increase at this time while GISP2 ssNa⁺ values remain level (Figs 2 and 3).

We suggest that the increase in marine air mass intrusion into West Antarctica (SD) and coastal East Antarctica (TD) is related to the ice dynamics/geographically controlled deglaciation of the Ross Sea Embayment previously described using glacial geologic features (Conway *et al.*, 1999). Both are coincident with an increase in atmospheric CO₂ (Fig. 3) which probably at this time, as it does today, led to changes in ice surface elevation and ice sheet extent through warming. As a consequence of this deglaciation the near circularity of the Antarctic ice sheet was disrupted between 12 000 and 5500 a BP as demonstrated by ice sheet model reconstructions (Fig. 4). During this period the Ross Sea Embayment became sufficiently prominent to significantly influence the inland penetration of the Amundsen Sea Low as is the case today (Lachlan-Cope *et al.*, 2001).

As change in SD ssNa⁺ plays a major role in our interpretation we provide additional validation for its role as an indicator of atmospheric circulation intensity and distance to an open ocean source (southward/northward migration of the ice front in the Ross Embayment) as follows. ssNa⁺ concentrations in Antarctic snow are controlled by elevation above and distance from the ocean (Bertler *et al.*, 2005) and strength of transport as noted previously (Kreutz *et al.*, 2000; Kaspari *et al.*, 2005). Elevation and distance inland to SD and TD have changed markedly since the deglaciation of the Ross Sea region (Fig. 4). To estimate the 'absolute maximum' lowering of the ice surface in the region of SD, assuming all ssNa⁺ change is due to elevation and therefore account for the elevation component of ssNa⁺ change over time, we compare SD ssNa⁺ concentration ~10 000 (SD a BP) with that of the highest value before the first major drop in SD ssNa⁺ in the Holocene at ~1000 (SD a BP) (Fig. 3). To calculate the 'absolute maximum' we use the Bertler *et al.* (2005) relationship developed from the ITASE spatial array of multi-year surface snow samples for ssNa⁺ and elevation where: elevation (in m a.s.l.) = $-495 \times \ln[\text{ssNa}^+ \text{ (in p.p.b.)}] + 4028$ ($r = -0.63$, $P < 0.001$). Concentrations of ssNa⁺ at ~10 000 and 1000 a are consistent with current values for ssNa⁺ found at elevations close to 2100 and 1650 m a.s.l., respectively, yielding an 'absolute maximum' drop in surface elevation of ~450 m to the present as SD today is at 621 m a.s.l. This is consistent with an estimate of ~350 m developed from a two-dimensional, full-stress, thermo-mechanical flow model (Price *et al.*, 2007) if all of the change in concentration is related to

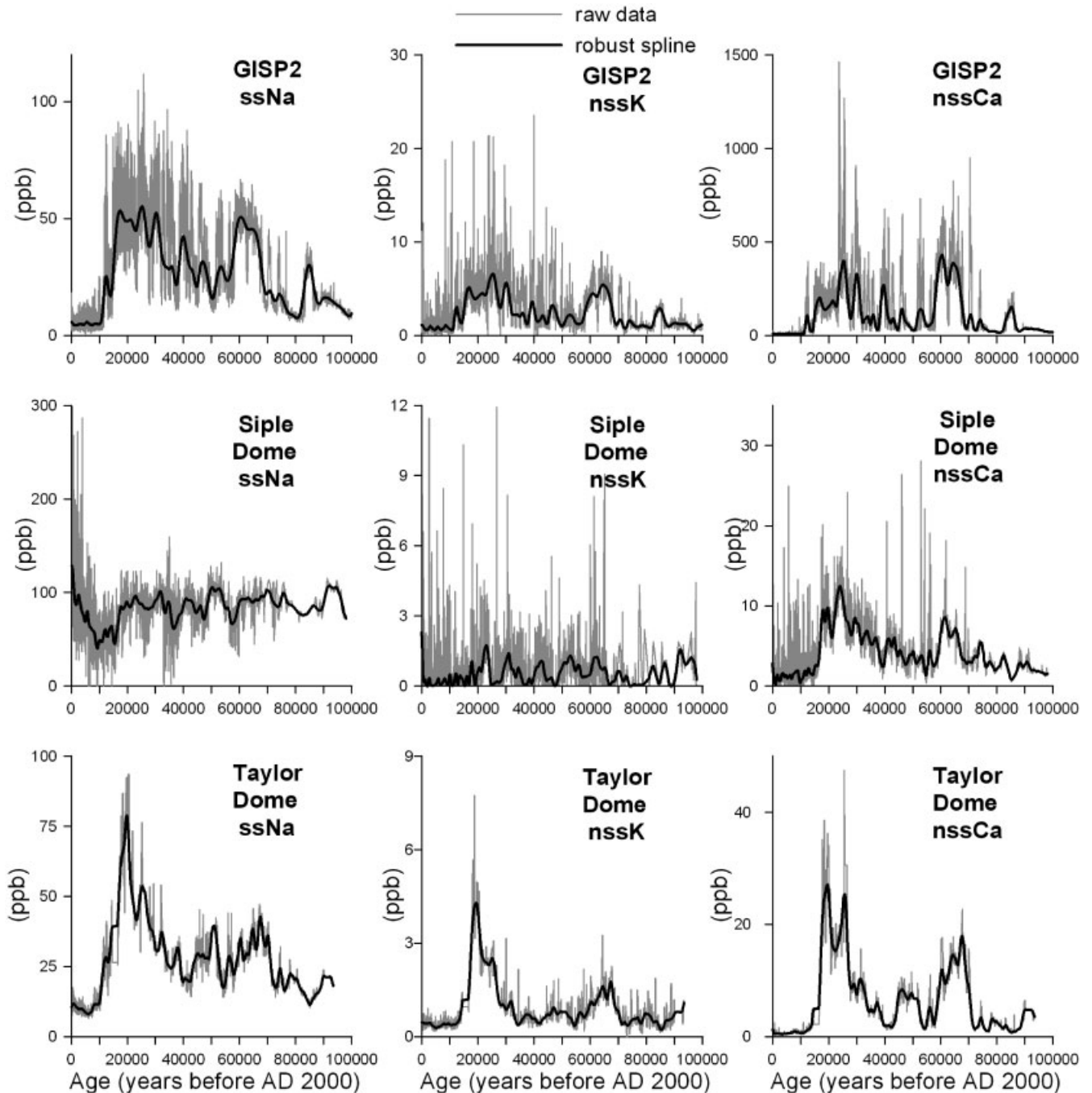


Figure 2. The last ~100 000 a of SD, GISP2 and TD ice core $ssNa^+$, $nssK^+$ and $nssCa^{2+}$ (all in p.p.b.) with raw data (gray) and robust smoothing spline (Meeker *et al.*, 1995) (black).

change in ice surface elevation. The Price *et al.* (2007) model invokes thinning ~14 000–15 000 (SD a BP) and we suggest based on the Conway *et al.* (1999) reconstruction that there was minimal impact at SD until the rise in SD $ssNa^+$ ~10 000 (SD a BP).

As of ~6000 (TD a BP) the increase in TD MS⁻ (Fig. 3) reveals a decrease in distance to the coast as the Ross Embayment continued to open and increase in SIE at the expense of grounded ice. Previous examination of TD and other East Antarctic ice cores suggests that ~5700 (TD a BP) marks the onset of a period of lower temperatures and expanded SIE throughout much of East Antarctica continuing through the Holocene (Steig *et al.*, 1998). In addition, temperature trends based on the $\delta^{18}O$ -temperature association diverge for SD (West Antarctica) and TD East Antarctica

as of ~6000 (SD a BP) (Fig. 3). We suggest that the rise in $\delta^{18}O$ SD and further inland in West Antarctica, based on the Byrd ice core record (Masson *et al.*, 2000), occurred in response to an increase in relatively warm marine air entering West Antarctica as a decrease in distance of transport alone without warming would probably bring more negative $\delta^{18}O$ -labeled air to SD, which would if anything reduce trends. The $\delta^{18}O$ rise is associated with continued retreat of grounded ice and lowering of ice surface elevations over the Ross Embayment coincident with CO_2 and CH_4 rise while East Antarctica remained relatively isolated from invading marine air. The same condition exists today, as evident by the relatively low $ssNa^+$ levels (minimal marine air mass penetration) characterizing East Antarctica (Bertler *et al.*, 2005).

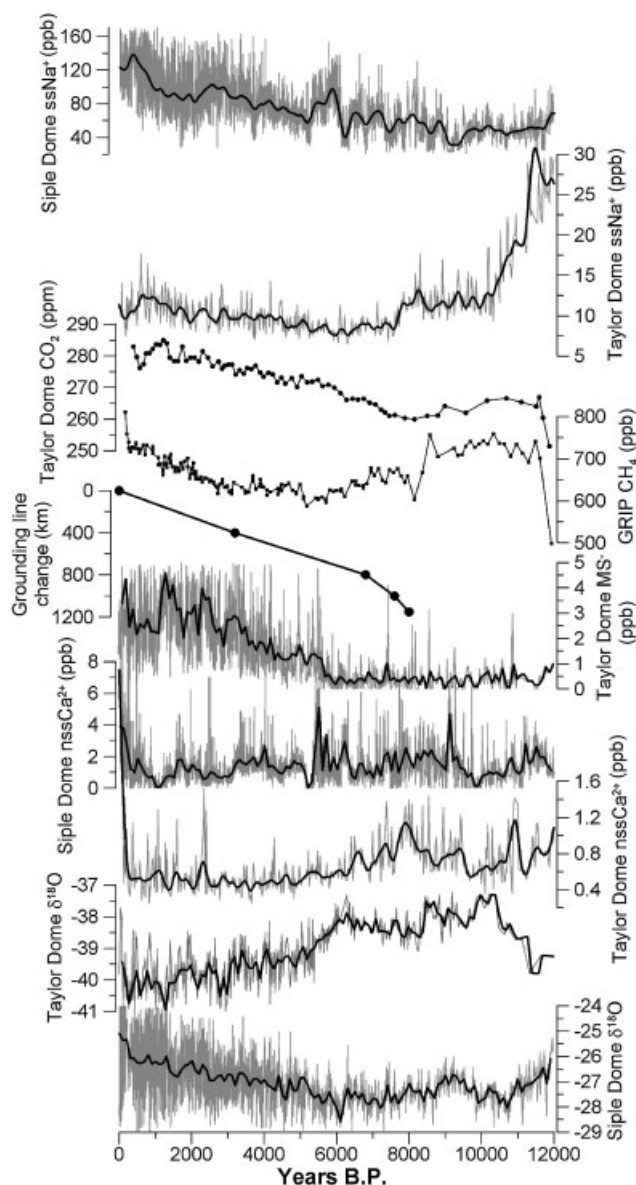


Figure 3. Raw (gray) and robust spline (black) time-series for SD $ssNa^+$ and $nssCa^{2+}$ and for TD MS^- (Steig *et al.*, 1998) covering the last 12 000 (SD and TD a BP) in addition to CO_2 (Indermuhle *et al.*, 1999), CH_4 (Blunier *et al.*, 1998), SD $\delta^{18}O$ (‰) and TD $\delta^{18}O$ (‰) (Steig *et al.*, 1998) and grounding-line retreat relative to the present Siple Coast at 3200, 6800 and 7600 cal a BP (black dots) in the Ross Embayment (Conway *et al.*, 1999).

Increased levels of SD and West Antarctic ITASE $nssCa^{2+}$ are associated with recent poleward migration of the austral westerlies (NAMIs) (Dixon *et al.*, 2011a). However, ~9000–10 000 until ~5500 (SD a BP) is also a period of high NAMI (increased SD and TD $nssCa^{2+}$) (Fig. 3). This period of higher NAMI resulted from the weaker thermal gradient and consequent increased meridional flow and greater inland penetration produced during relatively warm conditions prior to ~5500 (SD and TD a BP) over East Antarctica [as represented by TD $\delta^{18}O$ (Steig *et al.*, 1998)]. ~5500 (SD a BP) starts a marked decline in NAMI occurrence (decreased SD and TD $nssCa^{2+}$) coincident with the first major rise in CH_4 and continued rise of CO_2 and associated warming (Fig. 3) and increase in summer and winter insolation at 60°S (Mayewski *et al.*, 2004). The thermal gradient across the edge of the polar vortex steepened at this time in response to warming of

northerly regions, resulting in intensification of zonal flow and blocking of NAMIs. This steepened thermal gradient also resulted in divergence in temperature trends between West and East Antarctica isolating East Antarctica from warmer marine air masses. The dramatic divergence in East compared with West Antarctic temperatures demonstrates the impact of progressive polar contraction of the austral westerlies and increasing influence of the Amundsen Sea Low associated with Ross Sea Embayment deglaciation.

By ~5500 (SD a BP) West Antarctic and East Antarctic climate operate differently such that warming, ice loss and marine air mass invasion characterize West Antarctica while cooling dominates East Antarctica. This is similar to the situation in recent decades (Turner *et al.*, 2009b) except that the austral westerlies and associated lows were displaced notably farther north ~5500 (SD a BP) than today.

Holocene atmospheric reorganization

Detailed examination of the Holocene GISP2 chemistry record reveals marked periods of elevated marine ($ssNa^+$) and continental ($nssK^+$, $nssCa^{2+}$) source chemical species (Fig. 5) indicative of strengthening of both the Icelandic Low and the Siberian High (Meeker and Mayewski, 2002), respectively, and overall intensification of atmospheric circulation over the North Atlantic (O'Brien *et al.*, 1995; Mayewski *et al.*, 1997). Increases in SD $ssNa^+$ (strengthening of the Amundsen Sea Low) and increases in SD $nssK^+$ (extra-Antarctic air mass intensification) correspond to the major Holocene climate change events (Mayewski *et al.*, 2004) noted in GISP2 $ssNa^+$ and $nssK^+$ centered on ~8200, ~5700, ~2900, and ~400 (SD and GISP2 a BP) (Fig. 5). GISP2 and SD $nssCa^{2+}$ proxies for general intensification and/or proximity of the westerlies (O'Brien *et al.*, 1995) are synchronous within dating errors at ~5700 and ~600 (SD and GISP2 a BP) (Fig. 5).

Timing, global distribution and association with major climate forcings (insolation, CO_2 , CH_4 , solar variability and volcanic aerosols) of all of the foregoing events is demonstrated in an examination of 50 globally distributed paleoclimate time series (Mayewski *et al.*, 2004) and other studies (e.g. Renssen *et al.*, 2005; Bentley *et al.*, 2009) that do not include SD. Ice core proxies for the Amundsen Sea Low (SD $ssNa^+$) and the Icelandic Low (GISP2 $ssNa^+$) and westerlies (GISP2 and SD $nssCa^{2+}$) in the South Pacific and North Atlantic, respectively, reveal similar event timing, within dating errors, and similar abrupt onset and decay in $ssNa^+$, $nssK^+$ and $nssCa^{2+}$ for events centered on ~5700, ~8200 and ~400 (SD and GISP2 a BP) (Fig. 5). The close correspondence presented here for events from two ice core records (SD and GISP2) of similar dating quality and climate proxy calibration emphasizes the Arctic–Antarctic similarity of these events, supporting the significant forcing influence of solar variability (O'Brien *et al.*, 1995; Mayewski *et al.*, 2004, 2006). The TD record is not as well resolved and dated as SD and GISP2, but does demonstrate the significantly more subdued climate signature characteristic of East Antarctic ice core records (Fig. 5). The most prominent events in TD $ssNa^+$, $nssK^+$ and $nssCa^{2+}$ are centered at ~8200, ~2900 and ~400 (TD a BP).

The most recent 2000 a in the SD and GISP2 glaciochemical records are the most highly resolved (≤ 2.5 years per sample) portions in both records and the most accurately dated (Meese *et al.*, 1997; Taylor *et al.*, 2004). The most recent 1300 a in the TD record has relatively comparable resolution and dating (Steig *et al.*, 1998). As such, SD, GISP2 and TD provide a critical test for assessing timing and phasing of climate change over the last 2000 a where dating is highly precise and accurate.

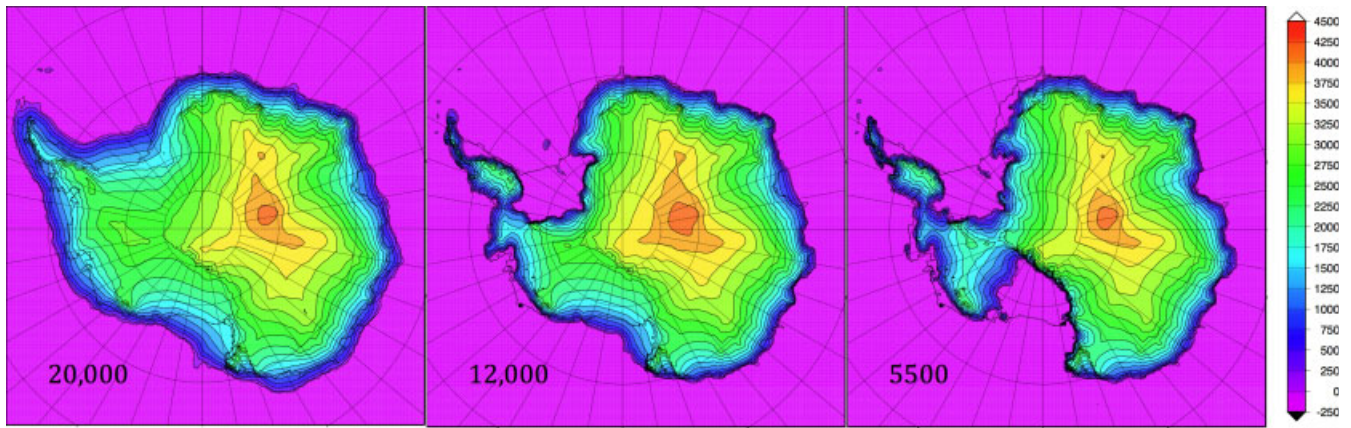


Figure 4. Antarctic ice sheet surface reconstructions demonstrating the decrease in extent of the ice sheet and the evolution of the Amundsen Sea Low for the periods 20 000, 12 000 and 5500 a BP generated using the University of Maine Ice Sheet Model (UMISM). The time slices shown here are from the spin-up runs of the SeaRISE (Sea-level Response to Ice Sheet Evolution) experiments. The model was run from 30 000 a BP to the present to provide time zero initial conditions for various perturbation runs attempting to assess the contribution to global sea level from Greenland and Antarctica. The data sets (bedrock topography, mass balance, surface temperature, geothermal flux, etc.) were provided by the SeaRISE community collected by Jesse Johnson at the University of Montana from various sources and are available at http://webserv.cs.umt.edu/isis/index.php/SeaRISE_Assessment.

The term Little Ice Age (LIA) is used to describe the most dramatic, pre-industrial era, change in temperature of the last 2000 a and one of the most prominent climate events of the last 5000 a (Mayewski *et al.*, 2004). New data from the Ross Sea sector of East Antarctica suggest that Antarctic sea and land surface temperatures were lower at this time (Bertler *et al.*, 2011).

In the GISP2 record the LIA is marked by the abrupt (<2.5 a) rise in $nssK^+$ ~600 (GISP2 a BP), followed by abrupt (<2.5 a) rise in $ssNa^+$ ~30 a later, then by an abrupt rise in $nssCa^{2+}$ another 10 a later marking, respectively and progressively, the onset of intensification of the Siberian High, the Icelandic Low and general zonal (boreal westerlies) flow (O'Brien *et al.*, 1995; Meeker and Mayewski, 2002; Mayewski and Maasch, 2006). The intensification of the Amundsen Sea Low (as indicated by SD $ssNa^+$), of NAMIs (SD $nssCa^{2+}$) and of SD $nssK^+$ starts ~1000–1500 (SD a BP), which is about 400–900 (SD a BP) before the intensification of atmospheric circulation over the North Atlantic (Mayewski and Maasch, 2006; Fig. 5). There is, however, a prominent break in SD $ssNa^+$ background levels coincident with the ~600 (SD a BP) abrupt event onset in the GISP2 record (Mayewski and Maasch, 2006; Fig. 5). The rise in SD $ssNa^+$ ~600 (SD a BP) appears less prominent as it is superimposed on a longer trend of SD $ssNa^+$ rise (Mayewski and Maasch, 2006; Fig. 5). The TD $ssNa^+$ record shows a rise similar in timing and structure to SD $ssNa^+$ associated with penetration of marine air masses into the Ross Embayment (Fig. 5).

Unlike SD $ssNa^+$ and SD $nssCa^{2+}$, SD $nssK^+$ increases abruptly ~400 (SD a BP), nearly 200 a after the abrupt rise in GISP2 $nssK^+$ and GISP2 $nssCa^{2+}$ (Fig. 5). Therefore, NAMIs containing $nssK^+$ source dust did not enter West Antarctica until ~400 (SD a BP). TD $nssK^+$ and $nssCa^{2+}$ do not rise until after the middle of the 20th century (Fig. 5), suggesting an even greater delay of dust-laden air masses into East Antarctica.

As of ~400 (SD a BP), $nssCa^{2+}$ and $ssNa^+$ operate inversely, suggesting stronger (weaker) westerlies and a shallower (deeper) Amundsen Sea Low until the last few decades. At this time SD $nssCa^{2+}$ and SD $ssNa^+$ operate more synchronously, intensifying and weakening in concert (Mayewski and Maasch, 2006), as the austral polar vortex and westerlies contract southward anchoring the Amundsen Sea Low closer to coastal West Antarctica. In the last few decades as the

westerlies and Amundsen Sea Low continue to contract southward, air masses laden with extra-Antarctic source dusts ($nssCa^{2+}$) have started to impact TD (Fig. 5).

In summary, the GISP2 (North Atlantic) and SD (South Pacific) ice core records are characterized by a near-coincident abrupt onset of atmospheric intensification ~600 (GISP2 and SD a BP) that in the case of SD is superimposed on a longer term decay of the Ross Embayment ice sheet.

Implications for the future

In recent decades, levels of TD $nssCa^{2+}$ and SD $nssCa^{2+}$ and SD $nssK^+$ are amongst the highest in the Holocene (Figs 3 and 5), demonstrating notable penetration of NAMIs into West Antarctica and coastal East Antarctica as the polar vortex and associated westerlies contract poleward (Fig. 1). NAMIs entering West Antarctica (SD $nssCa^{2+}$) increase as of ~150–200 (ITASE a BP) (Dixon *et al.*, 2011a) coincident with the onset of anthropogenic rise in greenhouse gases. The increase is unparalleled for the last ~5500 (SD a BP) prior to which NAMI events were prevalent in Antarctica because the thermal gradient across the edge of the polar vortex was weaker allowing NAMI penetration. In addition, SD $ssNa^+$ levels of the last 1000 (SD a BP) are the highest in the ~100 000-year-long SD ice core record (Fig. 2). Furthermore, current temperatures inferred from SD $\delta^{18}O$ are the highest in the SD record (ACCE, 2009). Finally, as a consequence of anthropogenic source emissions and increase in NAMIs, trace elements such as lead, cadmium and uranium have risen in the Antarctic atmosphere over recent decades (Dixon *et al.*, 2011b) exceeding even warm analog (Eemian interglacial) natural source trace element levels (Korotkikh *et al.*, 2011), further demonstrating the unique state of climate over Antarctica and the Southern Ocean over the last few decades (Turner *et al.*, 2009b; Mayewski *et al.*, 2009).

Antarctic climate variability is a product of changes in CO_2 , CH_4 , insolation and stratospheric ozone [related photochemically to solar irradiance (Shindell *et al.*, 1999; Mayewski *et al.*, 2006)] and, as of the advent of CFCs (chlorofluorocarbons), human source stratospheric ozone destruction in the southern hemisphere (Thompson and Solomon, 2002). All of the foregoing play a significant role in the intensity and location of major atmospheric circulation patterns by forcing changes in

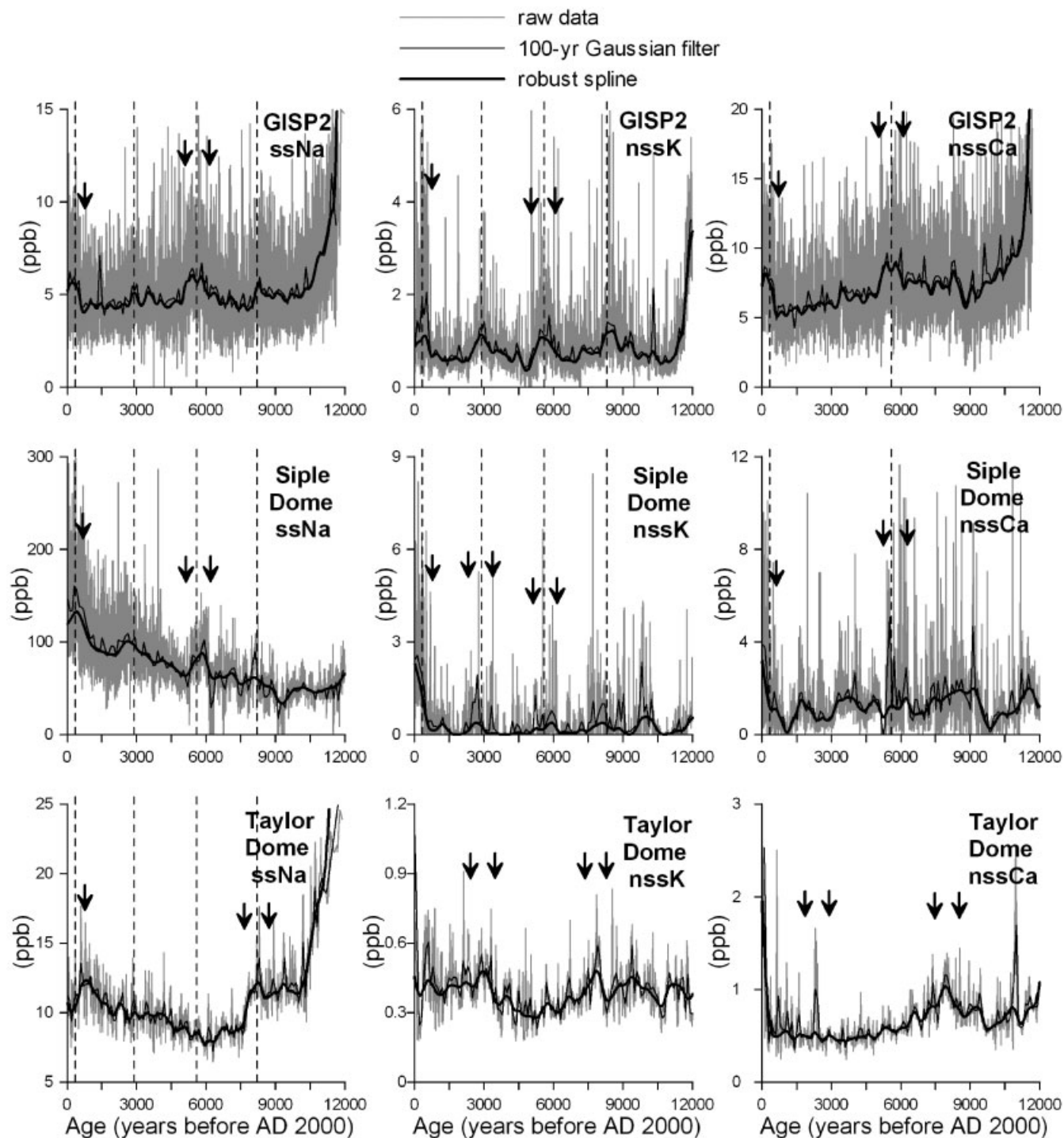


Figure 5. The last 12 000 a BP of ice core ssNa⁺, nssK⁺ and nssCa²⁺ from GISP2, SD and TD shown with raw data (gray line), 100-year Gaussian filter (thin black line), and low tension scale robust spline (heavy black line). Arrows and dotted vertical lines mark the general timing of the Holocene climate change events seen in GISP2 and in a globally distributed array of paleoclimate records (Mayewski *et al.*, 2004). Arrows mark periods of abrupt climate change (years to several years).

the thermal gradient of the atmosphere with consequent redistribution of heat and moisture. Understanding past variability in the position and intensity of the austral zonal westerlies and associated features such as the Amundsen Sea Low offers a tool for reconstructing climate variability over the Antarctic, the Southern Ocean, the southern hemisphere and globally. Paleo-reconstructions reveal dramatic expansions/contractions of the polar vortex and changes in intensity of circulation associated with the polar vortex over glacial/interglacial and millennial scales (Mayewski *et al.*, 1997; Shulmeister *et al.*, 2004; Shevenell *et al.*, 2011) and impacts on

precipitation variability during the Holocene throughout Africa, Asia and South America (Stager and Mayewski, 1997; Gasse, 2000).

Changes in the extent and duration of the polar vortex continue to play out today with the added impetus derived from human forcing of this system (Seidel *et al.*, 2008). As indicated by the SD nssCa²⁺ NAMI proxy record, changes in the strength of the austral westerlies and associated lows can start and end abruptly, within several years, superimposed on a polar vortex that has been contracting poleward in the region of West Antarctica over the Holocene as indicated by SD ssNa⁺ (Fig. 3).

The current state of West Antarctic climate is anomalous relative to the last ~100 000 a, meaning the polar vortex and westerlies are at their maximum southerly extent, allowing warm marine air in addition to extra-continental source dust-laden air into West Antarctica.

Most global and regional climate models suggest that poleward retreat of the austral westerlies will result from continued greenhouse warming during this century (Shulmeister *et al.*, 2004). Based on our results we suggest that continued greenhouse warming coupled with future healing of the Antarctic ozone hole will probably weaken the thermal gradient across the polar vortex, resulting potentially in abrupt disruptions to atmospheric circulation over the mid to high latitudes of at least the southern hemisphere. The implications of such changes are serious. As an example, winter storms borne on the austral westerlies are a major source of precipitation over southernmost Africa, Australia, New Zealand and South America and poleward migration of the northern margin of the westerlies tends to decrease rainfall in these regions (Shulmeister *et al.*, 2004; Reason and Rouault, 2005; van Ommen and Morgan, 2010; Lamy *et al.*, 2012; Stager *et al.*, 2012). These findings and our investigations point to the likelihood that the drying trend will continue in these regions and to the possibility that there will be in the future abrupt transitions in the continued poleward migration of the westerlies.

Acknowledgements. This research was supported by National Science Foundation Office of Polar Programs grants (0096305, 9316564, 0096299, 0424589, 0439589, 063740, 063650 and 0837883) and Brazilian National Council for Scientific and Technological Development part of the Brazilian Antarctic Program (PROANTAR), and the Chilean Antarctic Institute (INACH) and Fundación CEQUA. We gratefully acknowledge support from: the Polar Ice Coring Office (University of Alaska Fairbanks), Ice Core Drilling Services (University of Wisconsin Madison), the 109th Air National Guard (Scotia, New York), Chilean Air Force (FACH), Raytheon Polar Services, the National Ice Core Laboratory (NICL), analytical contributions from the Climate Change Research Center (University of New Hampshire) and E. A. Meyerson (Climate Change Institute), ice core drilling by M. Wumkes (Glacier Data), M. Gerasimov and M. Waskiewicz (Ice Core Drilling Services and the Polar Ice Coring Office), and our GISP2, Siple Dome, Taylor Dome and ITASE colleagues. GISP2, Siple Dome, Taylor Dome and ITASE are archived at National Climatic Data Center (NCDC).

Abbreviations. ITASE, International Trans Antarctic Scientific Expedition; LIA, Little Ice Age; NAMIs, northerly air mass incursions; nss, non-sea-salt; SIE, sea ice extent; ss, sea-salt.

References

- Bentley MJ, Hodgson DA, Smith JA, *et al.* 2009. Mechanisms of Holocene paleoenvironmental change in the Antarctic Peninsula region. *The Holocene* **19**: 51–69.
- Bertler NAN, Mayewski PA, Aristarain A, *et al.* 2005. Snow chemistry across Antarctica. *Ann. Glaciol.* **41**(1): 167–179.
- Bertler NAN, Mayewski PA, Carter L. 2011. Cold conditions in Antarctica during the Little Ice Age—Implications for abrupt climate change mechanisms. *Earth Planet. Sci. Lett.* DOI: 10.1016/j.epsl.2011.05.021.
- Blunier T, Chappellaz J, Schwander J, *et al.* 1998. Asynchrony of Antarctic and Greenland climate change during the last glacial period. *Nature* **394**: 739–743.
- Brook EJ, White JWC, Schilla ASM, *et al.* 2005. Timing of millennial-scale climate change at Siple Dome, West Antarctica, during the last glacial period. *Quaternary Sci. Rev.* **24**: 1333–1343.
- Conway H, Hall BL, Denton GH, *et al.* 1999. Past and future grounding-line retreat of West Antarctic Ice Sheet. *Science* **286**: 280–283.
- Delmonte B, Petit J-R, Andersen KK, *et al.* 2004. Dust size evidence for opposite regional atmospheric circulation changes over East Antarctica during the last climatic transition. *Climate Dynamics* **23**: 427–438.
- Divine DV, Koc N, Isaksson E, *et al.* 2009. Holocene Antarctic climate variability from ice and marine sediment cores: Insights on ocean-atmosphere interaction. *Quaternary Science Reviews* **29**: 303–312.
- Dixon DA, Mayewski PA, Goodwin I, *et al.* 2011a. An ice-core proxy for northerly air mass incursions into West Antarctica. *Int. J. Climatol.* DOI: 10.1002/joc.2371.
- Dixon DA, Mayewski PA, Korotkikh E, *et al.* 2011b. A spatial framework for assessing current conditions and monitoring future change in the chemistry of the Antarctic Atmosphere. *The Cryosphere Discuss.* **5**: 1–66. DOI: 10.5194/tcd-5-1-2011.
- Dixon DA, Mayewski PA, Kaspari SD, *et al.* 2005. A 200-year sulfate record from 16 Antarctic ice cores and associations with Southern Ocean sea ice extent. *Ann. Glaciol.* **41**: 155–166.
- Gasse F. 2000. Hydrological changes in the African tropics since the Last Glacial Maximum. *Quaternary Science Reviews* **19**: 189–211.
- Gille ST. 2002. Warming of the Southern Ocean since the 1950s. *Science* **95**(5558): 1275–1277.
- Hawley RL, Waddington ED, Morse DL, *et al.* (2002) Dating firn cores by vertical strain measurements, *J. Glaciol.* **48**: 401–406.
- Indermuhle A, Stocker TF, Joos F, *et al.* 1999. Holocene carbon-cycle dynamics based on CO₂ trapped in ice at Taylor Dome, Antarctica. *Nature* **398**: 121–126.
- Kaspari S, Mayewski PA, Dixon D, *et al.* 2005. Sources and transport pathways for marine aerosol species into West Antarctica. *Ann. Glaciol.* **41**: 1–9.
- Kreutz KJ, Mayewski PA, Pittalwala II, *et al.* 2000. Sea-level pressure variability in the Amundsen Sea region inferred from a West Antarctic glaciochemical record. *J. Geophys. Res.* **105**: 4047–4059.
- Korotkikh EV, Mayewski PA, Handley MJ, *et al.* 2011. The last interglacial as represented in the glaciochemical record from Mount Moulton Blue Ice Area, West Antarctica. *Quat. Sci. Rev.* **30**: 1940–1947. DOI: 10.1016/j.quascirev.2011.04.020.
- Lachlan-Cope TA, Connolley WM, Turner JT. 2001. The role of the nonaxisymmetric Antarctic orography in forcing the observed pattern of variability of the Antarctic climate. *Geophys. Res. Lett.* **28**: 4111–4114.
- Lamy F, Kilian R, Arz HW, *et al.* 2010. Holocene changes in the position and intensity of the southern westerly belt. *Nature Geosci* **3**: 695–699.
- Legrand M, Mayewski PA. 1997. Glaciochemistry of Polar ice cores: a review. *Rev. Geophys.* **35**: 219–243. DOI: 10.1029/96RG03527.
- Marshall GJ, Batista SD, Naik SS, *et al.* 2009. Analysis of a regional change in the sign of the SAM-temperature relationship in Antarctica. *Climate Dynamics*. DOI: 10.1007/s00382-009-0682-9.
- Masson V, Vimeux F, Jouzel J, *et al.* 2000. Holocene climate variability in Antarctica based on 11 ice-core isotopic records. *Quat. Res.* **54**: 348–358.
- Mayewski PA, Meeker LD, Twickler MS, *et al.* 1997. Major features and forcing of high-latitude northern hemisphere atmospheric circulation using a 110,000-year long glaciochemical series. *J. Geophys. Res.* **102**: 26, 345–26, 366.
- Mayewski PA, Rohling EE, Stager JC, *et al.* 2004. Holocene climate variability. *Quaternary Res.* **62**(3): 243–255.
- Mayewski PA, Maasch K, Yan Y, *et al.* 2006. Solar forcing of the polar atmosphere. *Ann. Glaciol.* **41**: 147–154.
- Mayewski PA, Maasch KA. 2006. Recent warming inconsistent with natural association between temperature and atmospheric circulation over the last 2000 years. *Clim. Past Discuss.* **23**: 327–355.
- Mayewski PA, Meredith M, Summerhayes C, *et al.* 2009. State of the Antarctic and Southern Ocean Climate System (SASOCS). *Rev. Geophys.* **47**: DOI: 10.1029/2007RG000231.
- Meeker LD, Mayewski PA. 2002. A 1400 year long record of atmospheric circulation over the North Atlantic and Asia. *The Holocene* **12**: 257–266.
- Meeker LD, Mayewski PA, Bloomfield P. 1995. A new approach to glaciochemical time series analysis. In *Ice Core Studies of Biogeochemical Cycles, NATO ASI Series*, vol. 130, RJ Delmas ed. Berlin; Springer: 383–400.

- Meese DA, Gow AJ, Alley RB, et al. 1997. The GISP2 depth-age scale: methods and results. *J. Geophys. Res.* **102**: 26, 411–26, 423.
- Mulvaney R, Röthlisberger R, Wolff EW, et al. 2000. The transition from the last glacial period in inland and near-coastal Antarctica. *Geophys. Res. Lett.* **27**: 2673–2676.
- O'Brien SR, Mayewski PA, Meeker LD, et al. 1995. Complexity of Holocene climate as reconstructed from a Greenland ice core. *Science* **270**: 1962–1964.
- Price SF, Conway H, Waddington ED. 2007. Evidence for late Pleistocene thinning of Siple Dome, West Antarctica. *J. Geophys. Res.* **112**: F03021. DOI: 10.1029/2006JF000725.
- Rankin AM, Auld V, Wolff EW. 2000. Frost flowers as a source of fractionated sea salt aerosol in the polar regions. *Geophys. Res. Lett.* **27**: 3469–3472.
- Reason CJC, Rouault M. 2005. Links between the Antarctic Oscillation and winter rainfall over western South Africa. *Geophys. Res. Lett.* **32**: L07705. DOI: 10.1029/2005GL022419.
- Renssen H, Goosse H, Fichefet T, et al. 2005. Holocene climate evolution in the high-latitude Southern Hemisphere simulated by a coupled atmosphere-sea ice-ocean-vegetation model. *The Holocene* **15**: 951–964.
- Schofield O, Ducklow HW, Martinson DG, et al. 2010. How do polar marine ecosystems respond to rapid climate change? *Science* **328**: 1520–1523.
- Seidel DJ, Qiang F, Randel WJ, et al. 2008. Widening of the tropical belt in a changing climate. *Nat. Geosci.* **1**: 21–24.
- Shevenell AE, Ingalls EA, Domack EW, et al. 2011. Holocene Southern Ocean surface temperature variability west of the Antarctic Peninsula. *Nature* **470**: 250–254.
- Shindell D, Rind D, Balachandran N, et al. 1999. Solar cycle variability, ozone and climate. *Science* **284**: 305–308.
- Shulmeister J, Goodwin I, Renwick J, et al. 2004. The Southern Hemisphere westerlies in the Australasian sector over the last glacial cycle: a synthesis. *Quat. Int.* **118–119**: 23–25.
- Sneed SB, Mayewski PA, Dixon 2011. An emerging technique: multi-ice core, multi-parameter correlations with Antarctic sea ice. *Ann. Glaciol.* **52**: 347–354.
- Stager JC, Mayewski PA. 1997. Abrupt mid-Holocene climatic transitions registered at the equator and the poles. *Science* **276**: 1834–1836.
- Stager JC, Mayewski PA, White J, et al. 2012. Rainfall variability in South Africa and Australia during the last millennium linked to meridional shifts in the austral westerlies. *Climates of the Past* **7**: 4375–4399.
- Steig EJ, Hart CP, White JWC, et al. 1998. Changes in climate, ocean and ice-sheet conditions in the Ross embayment, Antarctica at 6ka. *Ann. Glaciol.* **27**: 305–310.
- Taylor KC, Alley RB, Meese DA, et al. 2004. Dating the Siple Dome, Antarctica ice core by manual and computer interpretation of annual layering. *J. Glaciol.* **50**: 453–461.
- Thomas ER, Marshall GJ, McConnell JR. 2008. A doubling in snow accumulation in the western Antarctic Peninsula since 1850. *Geophys. Res. Lett.* **35**: L01706.
- Thompson DWJ, Solomon S. 2002. Interpretation of recent Southern Hemisphere climate change. *Science* **296**(5569): 895–899.
- Turner J, Lachlan-Cope TA, Colwell SR, et al. 2006. Significant warming of the Antarctic winter troposphere. *Science* **311**: 1914–1917.
- Turner J, Comiso JC, Marshall GJ, et al. 2009a. Non-annular atmospheric circulation change induced by stratospheric ozone depletion and its role in the recent increase of Antarctic sea ice extent. *Geophys. Res. Lett.* **36**: L08502.
- Turner TJ, Bindshadler R, Convey P, et al. (eds) 2009b. *Antarctic Climate Change and the Environment (ACCE)*. Cambridge.
- van Ommen TD, Morgan VI. 2010. Snowfall increase in coastal East Antarctica linked with southwest Western Australian drought. *Nature Geoscience* **3**: 267–272. DOI: 10.1038/NGE0761.
- Welch KA, Mayewski PA, Whitlow SI. 1993. Methanesulfonic acid in coastal Antarctic snow related to sea-ice extent. *Geophys. Res. Lett.* **20**: 443–446.
- Yan Y, Mayewski PA, Kang S, et al. 2005. An ice core proxy for Antarctic circumpolar wind intensity. *Ann. Glaciol.* **41**: 121–130.
- Yiou P, Fuhrer K, Meeker LD, et al. 1997. Paleoclimatic variability inferred from the spectral analysis of Greenland and Antarctic ice-core data. *J. Geophys. Res.* **102**: 26, 441–26,454.